Assessment of Ion Size Effects in the Diffuse Double Layer with Use of an Integral Equation Approach

ARTICLE *in* THE JOURNAL OF PHYSICAL CHEMISTRY B · MARCH 2005

Impact Factor: 3.3 · DOI: 10.1021/jp0475234 · Source: PubMed

2 AUTHORS, INCLUDING:

William Ronald Fawcett
University of California, Davis
87 PUBLICATIONS **1,593** CITATIONS

SEE PROFILE

Assessment of Ion Size Effects in the Diffuse Double Layer with Use of an Integral Equation Approach

W. Ronald Fawcett* and Thomas G. Smagala

Department of Chemistry, University of California, Davis, Davis, California 95616

Received: June 8, 2004; In Final Form: November 9, 2004

An analytical expression is developed for the potential drop across the diffuse layer φ^d in terms of a cubic polynomial in the corresponding estimate in the Gouy−Chapman approximation, φ^d(GC). The coefficients of this polynomial are defined in terms of the MSA volume fraction η and the reciprocal distance parameter Γ. The resulting expression is shown to describe the Monte Carlo estimates of φ^d obtained in a primitive level simulation of diffuse layer properties.

Introduction

The Gouy−Chapman (GC) model of the diffuse double layer is defective for several reasons, but mainly because it ignores the finite size of its component ions and their effects on the dielectric properties of the solvent. Some idea of the error in the GC estimate of the diffuse layer potential drop ϕ^d is obtained from Monte Carlo (MC) simulations at the primitive level.[1,2] On the basis of these calculations the GC estimate of ϕ^d is too large by an amount that depends on electrode charge density and electrolyte concentration. Similar conclusions are reached by using statistical mechanical theories based on the integral equation approach, for example, the hypernetted chain approximation (HNCA),[3] and by density functional theory.[1] The problem with all of these methods is that they do not lead to analytical expressions for the important diffuse layer properties including the value of ϕ^d.

An integral equation approach to the diffuse double layer problem that does lead to analytical expressions was developed recently by Fawcett at al.[4−6] Two corrections are found in terms of the functions Ξ_0 and H_0. The first of these depends on the volume fraction of the electrolyte solution that is occupied by the ions. The second function H_0 depends on the reciprocal distance Γ, which is defined in the mean spherical approximation (MSA), and is directly related to the more familiar Debye−Huckel reciprocal distance κ. Simple analytical functions are easily found for Ξ_0 and H_0 in the limit where the electrode's field is small. By using these expressions, an analytical expression can be written for the potential drop across the diffuse layer ϕ^d. It has already been shown[4−6] that the corresponding estimates of ϕ^d are close to the MC results. By modifying the functions Ξ_0 and H_0 in a minor way, an improved description of the MC results is possible with this approach.

In the present paper, the expressions for Ξ_0 and H_0 are reconsidered, and a model that approximately reproduces the MC results at the primitive level is described.

The Henderson−Blum (HB) Model

The description of the diffuse layer in the HNCA begins with the expressions for the ion-wall correlation functions at the outer Helmholtz plane (oHp). The wall-sum correlation function is

$$g^0_{ws} = \Xi_o \cosh[\varphi^d + H_0] \tag{1}$$

and the wall-difference correlation function is

$$g^o_{wd} = \Xi_o \sinh[\varphi^d + H_0] \tag{2}$$

The functions Ξ_0 and H_0 are defined in terms of integrals which contain either $g_{ws}(x)$ or $g_{wd}(x)$. In the HNCA, the values of $g_{ws}(x)$ and $g_{wd}(x)$ are initially based on the GCA. The calculation results in improved estimates of g^o_{ws} and g^o_{wd}. In the HNCA, these correlation functions are calculated by an iterative method until they are obtained to a satisfactory level of precision. In the noniterative approach described by Henderson and Blum,[2] the ion-wall correlation functions which result from using the GCA to estimate $g_{ws}(x)$ and $g_{wd}(x)$ are used without iteration. It was pointed out that the resulting values of Ξ_0 and H_0 should be reasonably good provided the field on the electrode and the electrolyte concentration are not too high. The calculations are carried out in terms of dimensionless quantities: the dimensionless field E is defined as

$$E = \sigma_m/A_{GC} \tag{3}$$

where σ_m is the electrode charge density, and A_{GC} is the Gouy−Chapman constant; the dimensionless diffuse layer potential drop is φ^d where

$$\varphi^d = F\phi^d/RT \tag{4}$$

The strategy adopted here, which is based on recent work,[6] is to limit the values of E to the range $-3 \le E \le 3$. This means that σ_m is limited to the range $-18 \le \sigma_m \le 18\ \mu C\ cm^{-2}$ for a 1 M solution of a 1−1 electrolyte. If the concentration falls to 0.01 M, the range of charge densities is dramatically reduced to $-1.8 \le \sigma_m \le 1.8\ \mu C\ cm^{-2}$. It is assumed that the noniterative procedure used by Henderson and Blum[2] is then relatively free of error. The functions derived for Ξ_0 and H_0 are based on calculations performed in this range, but are assumed to be valid for higher values of $|E|$.

The expressions for Ξ_0 and H_0 are based on definite integrals which have been given previously[4,5] and therefore are not

* Address correspondence to this author.

10.1021/jp0475234 CCC: $30.25
Published on Web 01/15/2005

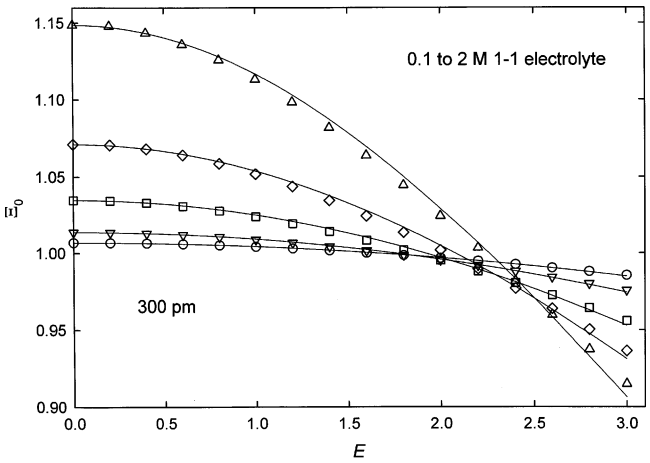

Figure 1. Plot of the HB function Ξ_0 against the dimensionless field E for a 1−1 electrolyte with concentrations of 0.1 (○), 0.2 (▽), 0.5 (□), 1 (◇), and 2 M (Δ) for an ion diameter of 300 pm. The solid curves show the least-squares fits of eq 5 to the data.

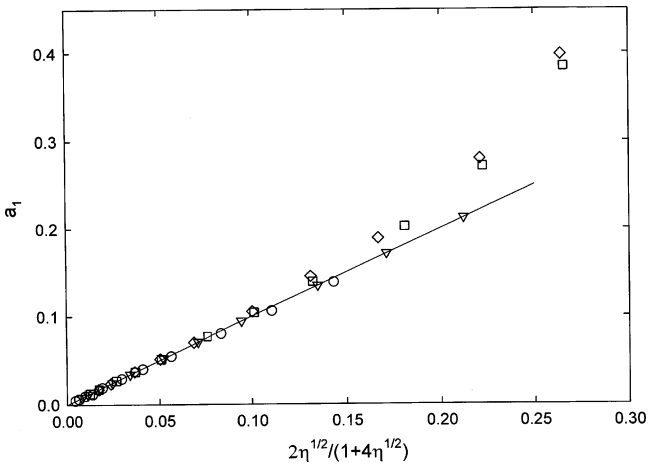

Figure 2. Plot of parameter a_1 determined from a least-squares fit of eq 5 to Ξ_0 data for ion diameters of 200 (○), 300 (Δ), and 400 pm (◇) against $2\eta^{1/2}/(1 + 4\eta^{1/2})$ estimated from the corresponding ionic volume fraction η.

repeated here. The function Ξ_0, which depends on the volume fraction η, is shown for the case that the ion size is 300 pm in Figure 1. This function is described to a good approximation by the equation

$$\Xi_o = a_0 \,\mathrm{sech}(a_1 E) \tag{5}$$

where

$$a_0 = \frac{1 + \eta + \eta^2 - \eta^3}{(1 - \eta)^3} \tag{6}$$

$$a_1 = \frac{2\eta^{1/2}}{1 + 4\eta^{1/2}} \tag{7}$$

and

$$\eta = \frac{2000 N_L \pi c_e \sigma^3}{6} \tag{8}$$

N_L is the Avogadro constant, c_e is the electrolyte concentration in M, and σ is the ion diameter in meters. The factor $2000N_L$ converts the electrolyte molarity to the number of ions per meter.[3] The diameters of the cations and anions are assumed to be the same; this corresponds to the restricted version of the HB model.

Values of a_1 determined in a least-squares fit of eq 5 to the estimated value of Ξ_0 are plotted against $2\eta^{1/2}/(1 + 4\eta^{1/2})$ in Figure 2. The solid line in this figure is drawn with unit slope. Eleven concentrations were considered in the range from 0.001 to 2 M, and three ion sizes, namely, 200, 300, and 400 pm. It is clear that eq 7 gives an accurate estimate of a_1 for low electrolyte concentrations but that the least-squares values fall above the HB estimate at higher concentrations. The fact that the data fall on one plot independent of ion size emphasizes that the assumption that the volume fraction η plays a role in determining the value of a_1 is correct.

The expression for the parameter a_0 is an improvement over the MSA estimate used in earlier work.[4−6] Equation 6 was obtained empirically by Carnahan and Starling[8] for a system of hard spheres. Its application to the present system represents an approximation.

The function H_0 was described in earlier work by the equation

$$H_0 = c_1 E + c_2 E^2 \tag{9}$$

However, as will be shown below, it can equally well be described by a cubic equation of the form

$$H_0 = c_1 E + c_3 E^3 \tag{10}$$

Because the functions involved in the final expression for φ^d can be expressed in infinite series involving odd powers of E, eq 10 is preferred over eq 9. The expressions for c_1 and c_3 are then given by

$$c_1 = \Gamma^2 \tag{11}$$

$$c_3 = \frac{\Gamma^{1.75}}{25(1 + \Gamma)^{1.75}} \tag{12}$$

where

$$\Gamma = \frac{(1 + 2\sigma\kappa)^{1/2}}{2} - \frac{1}{2} \tag{13}$$

and

$$\kappa = \left(\frac{2000 F^2 c_e}{\epsilon_o \epsilon_s RT}\right) \tag{14}$$

Here ϵ_s is the relative permittivity of the solvent at 25 °C (78.46) and ϵ_o is the permittivity of free space. The fit of eq 10 to data for H_0 estimated from the integral given earlier[4,5] by using the noniterative approach is shown in Figure 3. This simple cubic equation gives an excellent description of the results for values of $|E|$ less than 3.

Values of c_1 in eq 9 extracted from the least-squares data are plotted against the square of the MSA reciprocal distance Γ in Figure 4. Data at 200, 300, and 400 pm all fall on a straight line with unit slope. The fit applies over the concentration range up to 2 M so that eq 11 gives an excellent representation of the dependence of c_1 on ion size and concentration. The parameter c_3 is plotted against $[\Gamma/(1 + \Gamma)]^{1.75}$ in Figure 5. For lower values

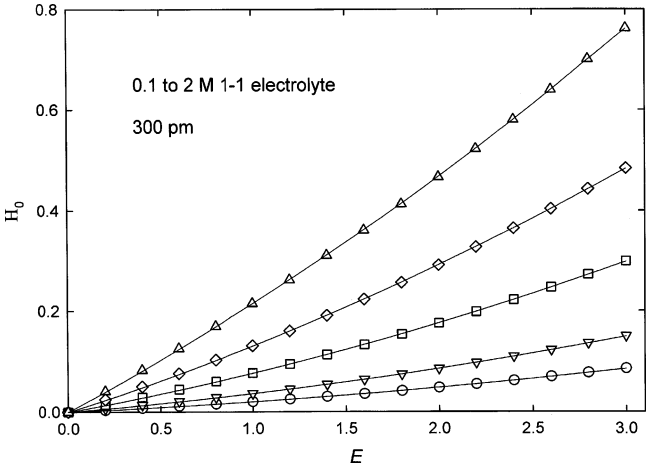

Figure 3. Plot of the HB function H_0 against the dimensionless field E for a 1−1 electrolyte with concentrations of 0.1 (○), 0.2 (▽), 0.5 (□), 1 (◇), and 2 M (△) for an ion diameter of 300 pm. The solid curves show the least-squares fits of eq 10 to the data.

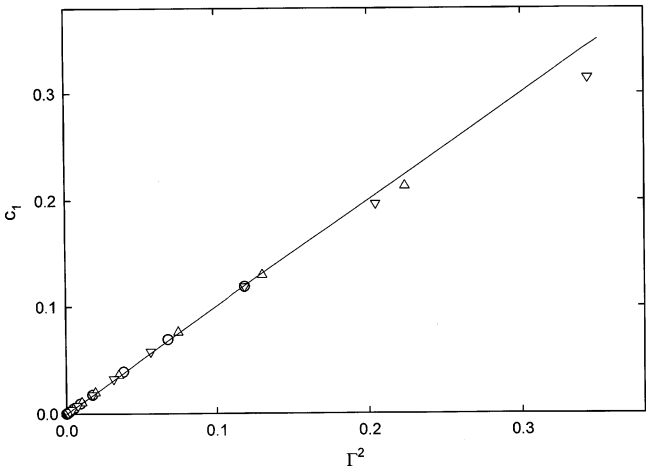

Figure 4. Plot of the parameter c_1 determined from a least-squares fit of eq 10 to H_0 data for ion diameters of 200 (○), 300 (◇), and 400 pm (△) against Γ^2 where Γ is the MSA reciprocal distance. The straight line is drawn with a slope of 1.00.

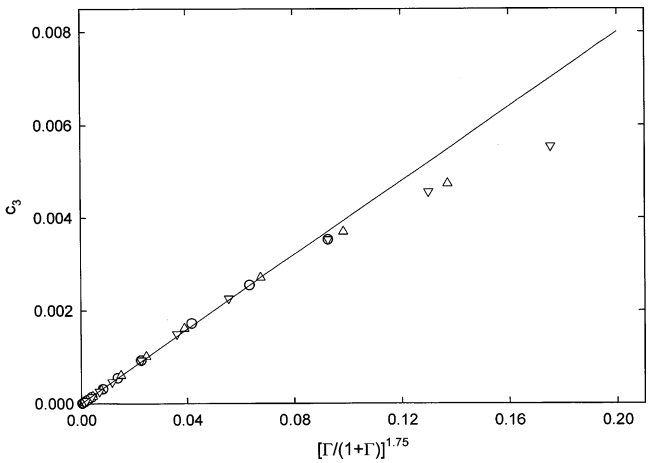

Figure 5. Plot of the parameter c_3 determined from a least-squares fit of eq 10 to H_0 data for ion diameters of 200 (○), 300 (▽), and 400 pm (□) against $[\Gamma/(1 + \Gamma)]^{1.75}$ where Γ is the MSA reciprocal distance parameter. The straight line is drawn with a slope of 0.04.

of c_3 there is a linear relationship between these quantities, but at higher values, the value of c_3 falls above the linear plot. The slope of the plot is 0.04 corresponding to eq 12.

Following HB,[3] the relationships between the ion-wall correlation functions at the oHp and the dimensionless field E are

$$g_{ws}^{o} = \Xi_o + E^2/2 \tag{15}$$

and

$$g_{wd}^{o} = E\left(\Xi_o + \frac{E^2}{4}\right)^{1/2} \tag{16}$$

Equation 15 is exact, and expresses the force balance condition at the interface.[3] On the basis of these equations, one may write

$$\cosh(\varphi^d + H_0) = 1 + \frac{E^2}{2\Xi^o} \tag{17}$$

and

$$\varphi^d = \cosh^{-1}\left[1 + \frac{E^2}{2a_0}\cosh(a_1 E)\right] - c_1 E - c_3 E^3 \tag{18}$$

φ^d is easily calculated in the HB model by using eq 18 with the estimates of a_0, a_1, c_1, and c_3 given above.

It is helpful to examine eq 18 in terms of an infinite series in E. Keeping in mind that the value of φ^d in the GCA is given by

$$\varphi^d(\mathrm{GC}) = \cosh^{-1}\left(1 + \frac{E^2}{2}\right) \tag{19}$$

and expanding the hyperbolic functions as an infinite series, one obtains for the difference $\varphi^d - \varphi^d(\mathrm{GC})$ the following expression:

$$\varphi^d - \varphi^d(\mathrm{GC}) = b_1 E + b_3 E^3 + b_5 E^5 + \ldots \tag{20}$$

The coefficients b_i become smaller with increasing powers of E so that under most circumstances only the first two coefficients b_1 and b_3 need to be considered in a fit of $\varphi^d - \varphi^d(\mathrm{GC})$ to E. The expressions obtained for b_1 and b_3 are

$$b_1 = -c_1 + \frac{1}{a_0^{1/2}} - 1 \tag{21}$$

and

$$b_3 = -c_3 + \frac{1}{24}\left(\frac{6a_1^2}{a_0^{1/2}} - \frac{1}{a_0^{3/2}} + 1\right) \tag{22}$$

It is also possible to express φ^d as an infinite series in powers of $\varphi^d(\mathrm{GC})$, that is,

$$\varphi^d = d_1\varphi^d(\mathrm{GC}) + d_3(\varphi^d(\mathrm{GC}))3 + d_5(\varphi^d(\mathrm{GC}))^5 + \ldots \tag{23}$$

The first two coefficients in this series are given by

$$d_1 = \frac{1}{a_0^{1/2}} - c_1 \tag{24}$$

and

$$d_3 = \frac{1}{24}\left[\frac{1}{a_0^{1/2}} + \frac{6a_1^2}{a_0^{1/2}} - \frac{1}{a_0^{3/2}} - c_1 - 24c_3\right] \tag{25}$$

The fact that only odd powers are involved in the series expansions in eqs 20 and 23 reveals an important property of the functions which define the oHp potential φ^d. For this reason, it is advantageous to fit the function H_0 to eq 10 rather than eq 9.

The Monte Carlo Calculations

The Monte Carlo (MC) calculations were carried out for a canonical ensemble, that is, for a fixed number of particles in a rectangular box of fixed volume at constant temperature. The ions were charged hard spheres in a dielectric continuum with a relative permittivity of 78.46 and temperature of 298.2 K. The system was contained in a rectangular box of length L with square ends that had dimensions of $W \times W$. One of the ends was charged with a uniform charge density equal to σ_m C m^{-2} and the other end uncharged. The number of cations in the box, n_+ , was not equal to the number of anions, n_- . The difference between them is determined by the charge on the wall. In addition, this difference is related to the dimensions of the square end $W \times W$, the relationship between W and Δn being

$$W = \left(\frac{10^{24} e_o \Delta n}{\sigma_m}\right)^{1/2} \tag{26}$$

where e_o is the fundamental charge and 10^{24} is a factor to convert m^2 to pm^2. For example, if σ_m is 0.2 C m^{-2} and Δn is 12, the value of W is 3,100 pm. On this basis, the end of the box is sufficiently large that statistical averaging to obtain the diffuse layer profiles is valid. The length of the box is chosen so that the average ion concentration in the central region far from the walls is equal to the desired bulk concentration. The value of L is initially estimated from the total number of ions by using the relationship

$$L = \frac{10^{33}(n_+ + n_-)}{2W^2 N_L c_e} \tag{27}$$

where N_L is the Avogadro constant, and c_e is the bulk electrolyte concentration in M. For $n_+ + n_-$ equal to 212, and $c_e = 1$ M, the estimate of L is 18,316 pm. The initial estimate is adjusted to achieve the desired bulk electrolyte concentration. For example, if the bulk concentration is too high, the box is made longer, thereby lowering the electrolyte concentration. The electrolyte concentration is easily adjusted in this way to the desired value to within one part in one thousand.

The program to carry out the MC calculations was written by Dr. Dezso Boda and has been applied to double layers in a variety of circumstances.[1,2,9−11]

Results and Discussion

Values of the potential drop across the diffuse layer φ^d were estimated by using eq 18 from the HB model with the values of a_0, a_1, c_1, and c_3 given by eqs 6, 7, 11, and 12, respectively. Estimates obtained for an electrolyte concentration of 1 M for three ionic diameters, namely, 200, 300, and 400 pm, are shown in Figure 6 where the values of φ^d are plotted against the GC estimate φ^d(GC). In all cases, the HB estimate is less than the GC value, the difference increasing with increase in ionic diameter. In addition, the value of φ^d reaches a maximum at higher charge densities and then begins to decrease. For an ionic diameter of 300 pm, the maximum value of φ^d (2.4) occurs for a charge density on the electrode of 30 μC cm^{-2}. Values of φ^d estimated in the MC simulations for $\sigma = 300$ pm are also shown in Figure 6. In this case there is no maximum in φ^d(MC), the estimates continuing to increase with increase in electrode charge density for the range considered ($\sigma_m \leq 40$ μC cm^{-2}). Although a small negative curvature is seen in the plot of φ^d(MC) against φ^d(GC), it is much less than that obtained with the HB approach. In fact the MC results are very well represented by the equation

$$\varphi_{MC}{}^d = d_1(\varphi_{GC}{}^d) + d_3(\varphi_{GC}{}^d)^3 \tag{28}$$

whereas the HB results require addition of a third term in (φ^d(GC)).[5]

MC results obtained for an electrolyte concentration of 1 M but with $\sigma = 200$ and 400 pm are shown in Figure 7. Two features can be observed when MC results are compared at the same concentration for changing ionic diameter. First of all, the initial slope of the plots of φ^d(MC) against φ^d(GC) decreases

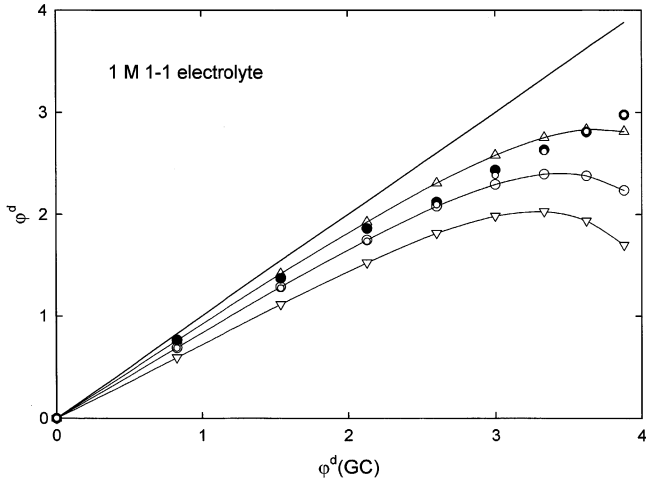

Figure 6. Plots of φ^d estimated by eq 18 with the values of the parameters a_0, a_1, c_1, and c_3 given by eqs 6, 7, 11, and 12, respectively, against the Gouy−Chapman value φ^d(GC) for ion diameters of 200 (Δ), 300 (○), and 400 pm (▽); the plot designated (●) gives the Monte Carlo results for an ionic diameter of 300 pm, and that designated (◊) gives the results obtained by using eq 28 with the parameters d_1 and d_3 given by eqs 34 and 35, respectively; the solid line gives the value of φ^d(GC) for reference.

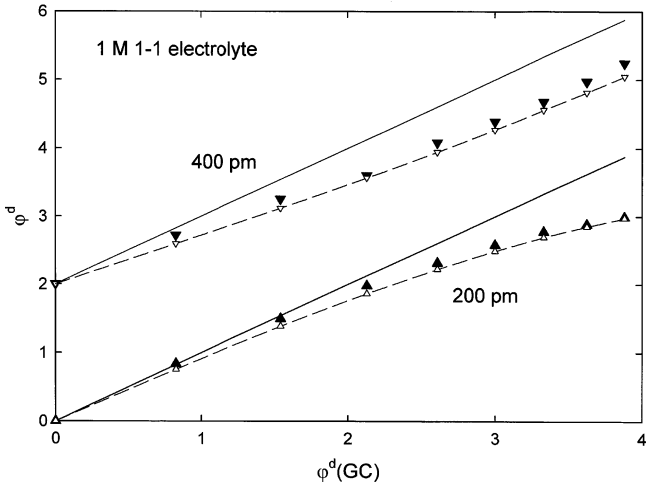

Figure 7. Plots of the Monte Carlo data for φ^d against the Gouy−Chapman value φ^d(GC) for a 1 M solution of a 1−1 electrolyte and for ion diameters of 200 (▲) and 400 pm (▼); the results designated as (Δ) and (▽) were obtained by using eq 28 with the parameters d_1 and d_3 given by eqs 34 and 35, respectively; the solid lines give the value of φ^d(GC) for reference; the results at 400 pm have been shifted vertically by 2 units for clarity.

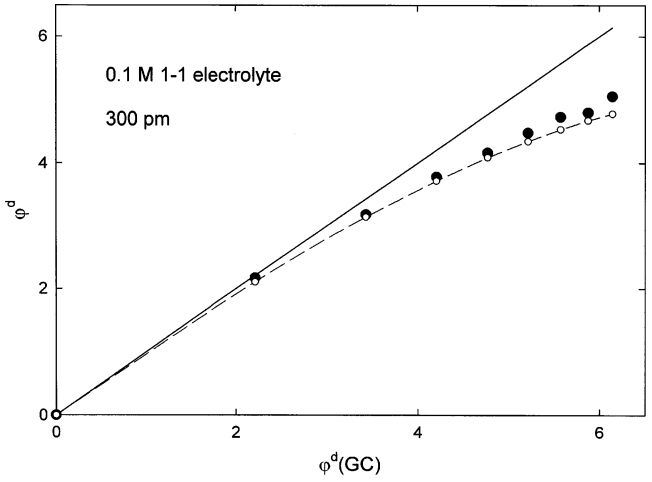

Figure 8. Plot of the Monte Carlo data for φ^d against the Gouy−Chapman value φ^d(GC) for a 0.1 M solution of a 1−1 electrolyte with an ion diameter of 300 pm (●); the results designated as (○) were obtained by using eq 28 with the parameters d_1 and d_3 given by eqs 34 and 35, respectively; the solid line gives the value of φ^d(GC) for reference.

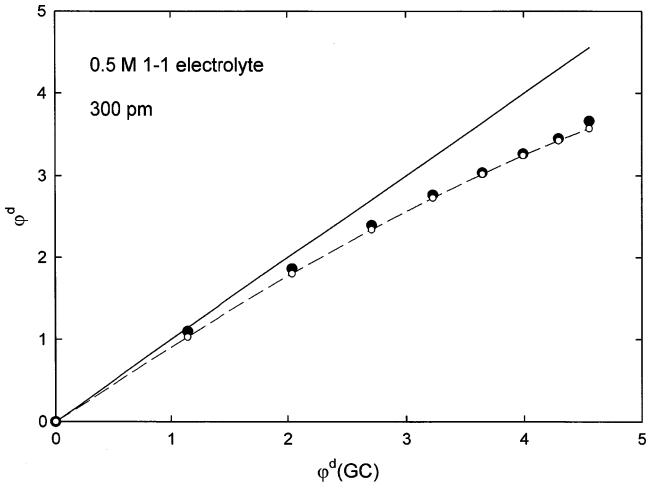

Figure 9. As in Figure 8 but for a 0.5 M solution of a 1−1 electrolyte.

with an increase in ion diameter. The second observation is that the curvature decreases in magnitude, being largest for $\sigma = 200$ pm and eventually reaching a small positive value for $\sigma = 400$ pm. Comparison with the HB results shown in Figure 6 shows that the trend in the curvature is exactly the opposite in this case, being small and negative for $\sigma = 200$ pm and increasing in magnitude with an increase in ionic diameter.

MC results for $\sigma = 300$ pm are shown in Figures 8−10 for electrolyte concentrations of 0.1, 0.5, and 2 M. In all cases, the dependence of φ^d(MC) on φ^d(GC) can be described by eq 28. The value of the initial slope d_1 decreases with an increase in electrolyte concentration. The curvature given by the coefficient d_3 is negative at the lower concentrations and eventually becomes positive at the highest concentration. When φ^d is estimated according to eq 18 the curvature is always negative and much greater than that found from the MC simulations.

Values of the parameters d_1 and d_3 were obtained by fitting the MC results to eq 28 for five concentrations, namely 0.1, 0.2, 0.5, 1.0, and 2.0 M for each of the ion diameters considered, namely 200, 300, and 400 pm. The results were then examined to see whether they are significant within the context of the HB approach. The first question is whether d_1 can be estimated by eq 24. Values of d_1 obtained in the two parameter least-

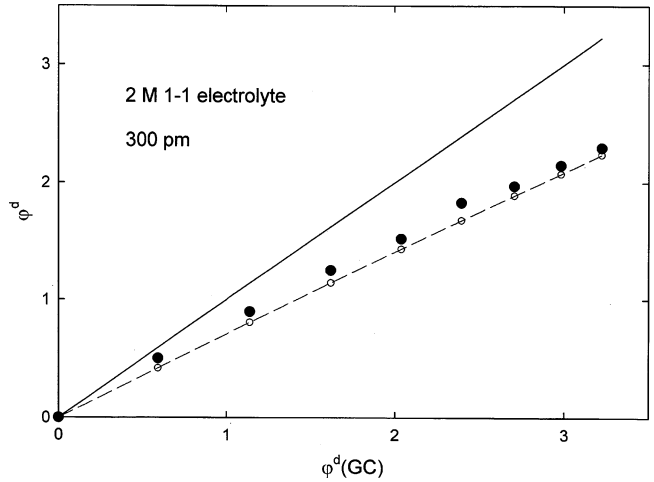

Figure 10. As in Figure 8 but for a 2 M solution of a 1−1 electrolyte.

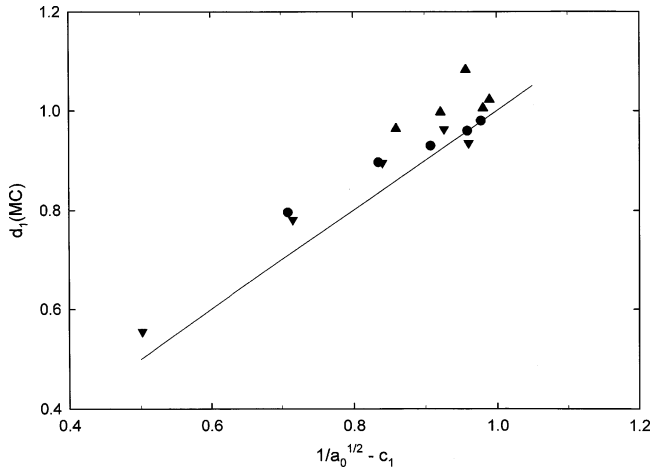

Figure 11. Plot of d_1 obtained by fitting eq 28 to Monte Carlo data obtained at five different concentrations and for three different ionic diameters against $(1/a_0)^{1/2} - \Gamma^2$; results are shown for 200 (▲), 300 (●), and 400 pm (▼); the solid line is drawn with a slope of one.

squares fit of eq 28 to the MC data obtained for 15 systems are shown in Figure 11. There is a tendency for the estimates of d_1 obtained from MC results to be too high but the maximum deviation between the value obtained from the MC data and eq 24 is never greater than 10%. Thus, it is reasonable to assume that d_1 is given by eq 24 to a very good approximation.

The MC data were then refitted to eq 28 in a one-parameter least-squares fit in which the values of d_1 were forced to be those given by eq 24. The resulting values of d_3 vary with both c_e and σ but no clear trend is apparent. This is due to the fact that d_3 is a complex function of four parameters defined above, namely, a_0, a_1, c_1, and c_3. Two of these parameters, a_0 and c_1, determine the linear coefficient d_1 and can be accepted as correct. However, the contributions of a_1 and c_3 must be reevaluated if the curvature coefficient d_3 is to be correctly estimated. Therefore, it is reasonable to evaluate a new curvature coefficient e_3 defined as

$$e_3 = d_3 - \frac{1}{24a_0^{1/2}} + \frac{1}{24a_0^{3/2}} + \frac{c_1}{24} = \frac{a_1^2}{4a^{1/2}} - c_3 \quad (29)$$

Values of e_3 are plotted against electrolyte concentration c_e in Figure 12. Clearly, e_3 increases with increase in electrolyte concentration but the change for $\sigma = 200$ pm is very small. In addition e_3 becomes positive for higher values of c_e and σ. This

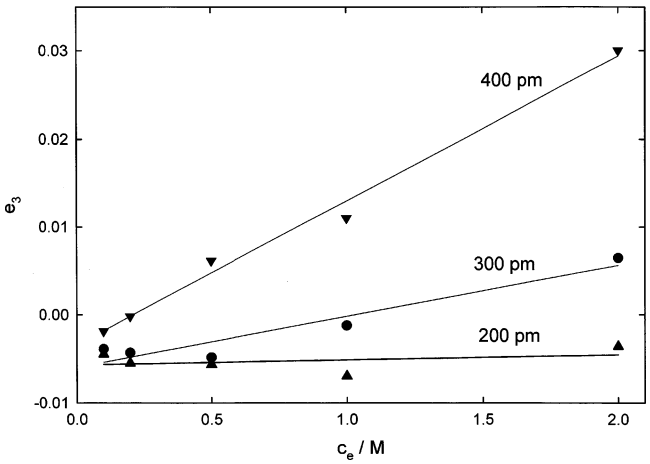

Figure 12. Plots of e_3 obtained from the Monte Carlo data (see eq 29) plotted against the electrolyte concentration; results are shown for 200 (▲), 300 (●), and 400 pm (▼).

means that the contribution from the term in a_1 must dominate under these conditions.

To optimize the values of the curvature parameter the MC data for e_3 were fit to the equation

$$e_3 = \alpha_1 f_1(\eta) + \alpha_2 f_2(\Gamma) \tag{30}$$

where $f_1(\eta)$ is a function of the volume fraction η, $f_2(\Gamma)$ is a function of the reciprocal distance parameter Γ, and α_1 and α_2 are numerical constants. Guided by the HB results various simple functions involving both integer and fractional powers of η and Γ were tested. The best fit to the MC results was obtained for the relationship

$$e_3 = \frac{\eta^{1/2}}{4a_0^{1/2}} - \frac{\Gamma}{8(1+\Gamma)} \tag{31}$$

Thus, we find that

$$a_1 = \eta^{1/4} \tag{32}$$

and

$$c_3 = \frac{\Gamma}{8(1+\Gamma)} \tag{33}$$

These results are very different from those obtained from the analysis of the HB functions Ξ_0 and H_0. This means that the HB approach can only be used in the limit of extremely small fields. Finally, the equations used to estimate the parameters d_1 and d_3 in the following discussion are

$$d_1 = \frac{1}{a_0^{1/2}} - \Gamma^2 \tag{34}$$

and

$$d_3 = \frac{1}{24a_0^{1/2}} + \frac{\eta^{1/2}}{4a_0^{1/2}} - \frac{1}{24a_0^{3/2}} - \frac{\Gamma^2}{24} - \frac{\Gamma}{8(1+\Gamma)} \tag{35}$$

where a_0 is given by eq 6.

The results obtained with eqs 34 and 35 with revised definitions of a_1 and c_3 are shown in Figures 6−10. It is clear that the revised results fit the MC data very well. Moreover, the revised estimates of φ^d are easily estimated from the GC value φ^d(GC) once the volume fraction η and the reciprocal distance parameter Γ have been estimated. Thus, the present approach gives a simple analytical equation that can be used to estimate the diffuse layer potential with consideration of ion size effects. In the case of 1−1 electrolytes, the corrections to the GC estimates of φ^d are important at high concentrations and electrode charge densities. The failure of the GC model is much more important for 2−1, 1−2, and 2−2 electrolytes. Application of the present approach to these systems will be considered in a future paper.

It is important to reiterate the limitations of the MC system used to generate the data used in the present analysis. In the primitive level description of the system used here, the dielectric permittivity is assumed to be uniform throughout the double layer. It would be interesting to carry out MC simulations with a dielectric layer at the interface with a much lower permittivity than that in the diffuse layer. The effect of images in the electrode phase should also be considered. Finally, the addition of electrolyte to the system lowers the permittivity of the solution with respect to that of the pure solvent.[12] This effect should also be considered in an improvement of the primitive level model.

However, the major effects of finite ion size on diffuse layer properties are undoubtedly included in the results used to generate the present analytical model.

Acknowledgment. The financial support of the National Science Foundation (CHE 0133758) is gratefully acknowledged.

References and Notes

(1) Boda, D.; Fawcett, W. R.; Henderson, D.; Sokolowski, S. *J. Chem. Phys.* **2002**, *116*, 7170.
(2) Boda, D.; Henderson, D.; Plaschko, P.; Fawcett, W. R. *Mol. Simul.* **2004**, *30*, 137.
(3) Henderson, D.; Blum, L. *J. Electroanal. Chem.* **1980**, *111*, 217.
(4) Fawcett, W. R.; Henderson, D. *J. Phys. Chem. B* **2000**, *104*, 6837.
(5) Fawcett, W. R. *Russ. J. Electrochem.* **2002**, *38*, 2.
(6) Andreu, R.; Fawcett, W. R. *J. Electroanal. Chem.* **2003**, *552*, 105.
(7) Henderson, D.; Blum, L. *Can. J. Chem.* **1981**, *59*, 1906.
(8) Carnahan, N. F.; Starling, K. E. *J. Chem. Phys.* **1970**, *53*, 600.
(9) Boda, D.; Chan, K.-Y.; Henderson, D. *J. Chem. Phys.* **1998**, *109*, 7362.
(10) Boda, D.; Henderson, D.; Chan, K.-Y. *J. Chem. Phys.* **1999**, *110*, 5346.
(11) Boda, D.; Henderson, D.; Busath, D. D. *J. Phys. Chem. B* **2001**, *105*, 11574.
(12) Fawcett, W. R. *Liquids, Solutions, and Interfaces*; Oxford University Press: New York, 2004; Chapter 4.